HHS Public Access

Author manuscript

J Mol Cell Cardiol. Author manuscript; available in PMC 2016 March 01.

Published in final edited form as:

J Mol Cell Cardiol. 2015 March ; 80: 175–185. doi:10.1016/j.yjmcc.2015.01.006.

Reciprocal interactions between mitral valve endothelial and interstitial cells reduce endothelial-to-mesenchymal transition and myofibroblastic activation

Kayle Shapero[1,2], **Jill Wylie-Sears**[1], **Robert A. Levine**[3], **John E. Mayer Jr**, and **Joyce Bischoff**[1]

[1]Vascular Biology Program and Department of Surgery, Boston Children's Hospital, and Harvard Medical School, Boston University, Boston, MA

[2]Biomedical Engineering Department, Boston University, Boston, MA

[3]Cardiac Ultrasound Laboratory, Massachusetts General Hospital β1Hospital and Harvard Medical School, Boston, MA 02115

Abstract

Thickening of mitral leaflets, endothelial-to-mesenchymal transition (EndMT), and activated myofibroblast-like interstitial cells have been observed in ischemic mitral valve regurgitation. We set out to determine if interactions between mitral valve endothelial cells (VEC) and interstitial cells (VIC) might affect these alterations. We used in vitro co-culture in Transwell™ inserts to test the hypothesis that VIC secrete factors that inhibit EndMT and conversely, that VEC secrete factors that mitigate the activation of VIC to a myofibroblast-like, activated phenotype. Primary cultures and clonal populations of ovine mitral VIC and VEC were used. Western blot, quantitative reverse transcriptase PCR (qPCR) and functional assays were used to assess changes in cell phenotype and behavior. VIC or conditioned media from VIC inhibited transforming growth factorβ (TGFβ)-induced EndMT in VEC, as indicated by reduced expression of EndMT markers α-smooth muscle actin (α-SMA), Slug, Snai1 and MMP-2 and maintained ability of VEC to mediate leukocyte adhesion, an important endothelial function. VEC or conditioned media from VEC reversed the spontaneous cell culture-induced change in VIC to an activated phenotype, as indicated by reduced expression of α-SMA and type I collagen, increased expression chondromodulin-1 (Chm1), and reduced contractile activity. These results demonstrate that mitral VEC and VIC secrete soluble factors that can reduce VIC activation and inhibit TGFβ-driven EndMT, respectively. These findings suggest that the endothelium of the mitral valve is critical for

Corresponding author: Joyce Bischoff, Ph.D., Vascular Biology Program, Karp Family Research Building 12.212, Boston Children's Hospital, Boston, MA 02115, Phone: 617-919-2192, joyce.bischoff@childrens.harvard.edu.

Disclosures

None.

the maintenance of a quiescent VIC phenotype and that, in turn, VIC prevent EndMT. We speculate that disturbance of the ongoing reciprocal interactions between VEC and VICs *in vivo* may contribute to the thickened and fibrotic leaflets observed in ischemic mitral regurgitation, and in other types of valve disease.

Keywords

mitral valve; endothelial cells; endothelial-to-mesenchymal transition; valve interstitial cells

1. Introduction

Many mitral valve pathologies, including ischemic mitral regurgitation, are characterized by thickened valve leaflets, myofibroblastic-like interstitial cells, disrupted extracellular matrix (ECM)[1, 2], and in some, evidence for endothelial-to-mesenchymal transition (EndMT)[3]. The cellular mechanisms that normally prevent these alterations are not well-understood. Here we set out to examine how mitral valve endothelial cells (VEC) and interstitial cells (VIC) might interact with each other to maintain quiescent VEC and VIC phenotypes that are observed in healthy valves [4, 5].

The mitral valve endothelium is continuous and uniformly positive for the endothelial markers CD31 [3] and von Willebrand Factor [6]. The integrity of the endothelium is thought to be critical for durability and function of the mitral valve over a lifetime [7]. Emerging evidence suggests that subsets of VEC are progenitor cells that appear and function as endothelium but can be stimulated to undergo EndMT, and further to express markers of osteogenic and chondrogenic mesenchymal cells [8, 9]. The onset and function of EndMT in adult valves is not well understood. We speculated in previous work that low levels of EndMT may serve to replenish the VIC population over a lifetime [10, 11]. More recently, we found increased EndMT in ovine mitral valve leaflets exposed to mechanical tethering in a model designed to mimic the mechanical stretch imposed on the mitral valve after myocardial infarction [3]. This finding implicated EndMT as an adaptive mechanism that may contribute to increased mitral leaflet thickness and area in this ovine model [3]. These studies point to a dynamic role for the endothelium in mitral valve homeostasis and adaptation.

As primary biosynthetic producers of the ECM, the mitral VIC play a critical role in maintaining the structural integrity of the leaflets, which must form an effective seal in systole to prevent mitral regurgitation. VIC resemble fibroblasts but exhibit considerable heterogeneity that is not yet defined by specific markers. Three types of VICs have been proposed: quiescent VIC, activated VIC and progenitor-like VIC [5]. Quiescent VIC produce basal levels of ECM tailored to the specific layer in which the VIC resides – the atrialis, spongiosa or fibrosa [12]. Chondromodulin1 (Chm1), a 25kDa secreted glycoprotein, is prominently expressed in avascular regions of cardiac valves wherein it prevents angiogenesis [13]. Excessive angiogenesis is often correlated with disrupted heart valve function and disease. Thus, Chm1 serves as a marker of healthy valves. In contrast, α-SMA-positive VIC are increased in diseased valves [14, 15].

In culture, mitral VEC form cobblestone monolayers, express CD31, vascular endothelial (VE)-cadherin [9] and von Willebrand Factor [6]. Flanagan and colleagues showed that porcine mitral VEC express ECM components but unlike VIC, do not express type I collagen [6]. As observed with VEC from pulmonary and aortic valves [9–11, 16, 17], mitral VEC undergo EndMT when treated with TGFβ [9]. Taken together, the ability of VEC to undergo EndMT in response to mechanical stimuli [3, 18], inflammatory cytokines [19] as well as TGFβ, points to a dynamic endothelium overlying the VIC.

In culture, VIC adopt an activated phenotype, characterized primarily by α-SMA expression in 30–100% of the cells, a finding which has been attributed to the rigidity of the plastic substratum [20, 21]. Activated VIC also display contractile activity [22] indicative of the myofibroblastic phenotype. In vitro, *mitral* VIC have been shown to express α-SMA, vimentin [23], type I collagen [6] and Chm1 [24]. VICs can be induced to an activated phenotype by a variety of mechanisms, including chemical stimuli [12] [25–29], substrate stiffness [20, 30], and mechanical stimulation (shear stress or stretching) [22, 31–33].

We hypothesize that normal valve cellular and ECM integrity is actively maintained in homeostatic balance by paracrine interactions between VIC and VEC that inhibit EndMT and suppress VIC activation. Previous observations show that VEC communicate effectively with one another via surface receptors and can influence one another's phenotypes [34, 35]. There are also studies that show VEC-generated nitric oxide reduces calcification and activation of aortic VIC [36–38]. To address our hypothesis, we used an in vitro indirect co-culture assay to determine if mitral VEC and VIC can modulate one another under defined conditions but in the absence of additional stimuli such as mechanical forces.

2. Materials and Methods

2.1 Materials

Used were Endothelial Basal Medium (EBM)-2 (CC-3156, Lonza, Hopkinton, MA); fetal bovine serum (FBS) (Hyclone, Logan, UT); Glutamine-penicillin-streptomycin sulfate (GPS) DNase I, Amplification Grade and Cell Titer96 Aqueous One Solution Cell Proliferation Assay (Life Technologies (formerly Invitrogen), Carlsbad, California); tumor necrosis factor alpha (TNF-α), human TGFβ-1 (100-B-001) (R&D Systems, Minneapolis, MN), basic fibroblast growth factor (11123149001) (Roche Diagnostics, Indianapolis, IN), fluorescein isothiocyanate (FITC) anti-goat IgG (FI-5000), Texas Red anti-mouse immunoglobulin G (IgG) (TI-2000), peroxidase conjugated anti-mouse IgG (PI-2000), peroxidase conjugated anti-goat IgG (PI-9500) (Vector Laboratories, Burlingame, CA), FITC-conjugated anti-human CD31 (SC-1506) (Ancell, Bayport, MN), mouse anti-human α-SMA (A-2547, Sigma Aldrich Co., St. Louis, MO), goat anti-human CD31 (SC-1506), goat anti-human vascular endothelial-Cadherin (VE-Cadherin) (SC-6458) (Santa Cruz Biotechnology, Santa Cruz, CA), mouse anti-bovine endothelial nitric oxide synthase (eNOS) (clone 9D10, 33-4600, Life Technologies), rabbit antihuman von Willebrand Factor (vWF) (A-0082), rabbit polyclonal anti-vimentin antibody (Ab-45939), smooth muscle myosin heavy chain alpha (SM22alpha) (Ab-10135) (Abcam, Cambridge, MA), FITC-streptavidin (SA-5001) and Texas Red-streptavidin (SA-5006) (Amersham Life Sciences, Arlington Heights, IL), RNeasy kit and RNase-free DNase (Qiagen, Valencia, CA),

Collagenase A (Roche Diagnostics, Indianapolis, IN), Type I collagen (Cohesion Technologies Inc., Palo Alto, CA and BD Biosciences, Bedford MA), phenol red-free Matrigel (BD Biosciences, Bedford, MA). Immobilon-P membrane (Millipore, Bedford, MA), Hyperfilm ECL, 24mm Transwells with 0.4μm pore polycarbonate membrane inserts, 12mm Transwells with 0.4μm pore polycarbonate membrane inserts, (Corning Life Sciences, Acton, MA).

2.2 Mitral Valve Cell Isolation, Culture and Clonal Populations

Ovine mitral valves and carotid arteries were obtained from animals weighing 20 to 25 kg and 8 to 10 months of age under approved guidelines for animal experimentation. Valve leaflets were incubated in EBM-2 media with 5% FBS, 1% GPS, 2 mmol/L L-glutamine, and 100 μg/ml gentamicin sulfate for 1 to 4 hours, minced into 2 mm^2 pieces, incubated with 0.2% collagenase A in EBM-2 media for 5 minutes at 37°C, and diluted with Hanks' balanced salt solution containing 5% FBS, 1.26 mmol/L $CaCl_2$, 0.8 mmol/L $MgSO_4$, and 1% GPS (wash buffer). The supernatant from the digest was sedimented at 200 × *g*, resuspended in EBM-B media (EBM-2 media, 10% heat-inactivated FBS, 1% GPS, and 2 ng/mL basic fibroblast growth factor) and plated. The following day, primary cultures were washed to remove unattached cells and given fresh EBM-B. To prepare clonal populations, primary cultures were expanded for approximately 7 days, trypsinized, resuspended in EBM-B at 3.3 cells/ml, and 100 μl was plated in each well of a 96-well plate; visual inspection was performed to verify that single colonies appeared in a subset of wells. When the colonies covered two-thirds of the well, cells were split into 24-well dishes. The mitral VEC clones were characterized as previously described [9] and designated mitral VEC-4, VEC-5, VEC-E10.

Interstitial cells were expanded from the same collagenase digest and designated as mitral VIC-7, VIC-G8, and VIC-B12. Two additional clones, mitral VIC-K5 and VIC-K19 were isolated from a second preparation from the same leaflet. Larger pieces of leaflet tissue were cultured on a gelatin-coated plate for 1–2 weeks. Interstitial cells migrated directly out from the leaflet tissue and once the cells covered two-thirds of the plate, clonal populations were prepared using the single cell isolation procedure described listed above, and expanded from 96 wells plates.

Both mitral VEC and VIC cells were expanded on 1% gelatin-coated dishes in EBM-B and both cell types were passaged 1:3 or 1:4 every 6 to 14 days and used between passages 8 to 14. In some experiments the primary culture of mitral VIC was used (isolated just prior to preparation of the clones), and these cells were used between passages 2–5.

2.3 Non-Valvular Cells

Ovine carotid artery endothelial cells (CAEC) were isolated as described by collagenase (0.2% vol/vol final) and dispase (2.5 U/mL final) digestion for 1 hour at 37°C[9]. Sheep endothelial colony forming cells (ECFCs) were isolated from peripheral blood samples as described [39]. Ovine bone marrow-derived mesenchymal stem cells (BM-MSC) were isolated as described [40]. Fibrocytes were isolated from human peripheral blood mononuclear cells [41]. Non-valvular ECs are not transformed cell lines. For experiments in

this study, they were grown in EBM-B under identical conditions as the mitral VEC and VIC.

2.4 Endothelial to Mesenchymal Transition (EndMT) Assay

Cells were grown in EBM-B or EBM-B with 2 ng/ml of $TGF\beta_1$ for four to five days. The media was replaced every two to three days. Upon completion of the experiment the cells were lysed and prepared for Western Blot, RNA extraction, or indirect immunofluorescence. Previous studies showed that ovine aortic VEC undergo EndMT in response to all three TGFβ isoforms and that VEC express TGFβ receptors [10, 11].

2.5 Co-culture/Conditioned Media (CM) Assays

For the co-culture experiments, cells were plated either in the insert or the bottom of 6 well Transwell™ plates at a density of 1×10^4 cells/cm^2, and allowed to adhere overnight. After 24 h the two cell types were placed in indirect co-culture by overlaying the inserts in wells containing the target cell. The co-cultures were treated for the specified times in EBM-B supplemented with $TGF\beta_1$, as noted for each experiment. For CM experiments, cells were treated with CM that had been produced by the specified cell type for 24 h, at which point it was sterile filtered and added in a 1:1 ratio with fresh media to target cells. Media was replaced with fresh CM every 2–3 days.

2.6 Flow Cytometry

Ovine cells were removed from the culture plate with Cell Dissociation Buffer, (Gibco, Life Technologies, Grand Island, NY) fixed for 30 min in 4% paraformaldehyde, followed by 10 min in 0.5% saponin in 1% BSA/PBS. Cells were then washed and incubated with PE or FITC-conjugated Abs (anti-CD31 or anti-α-SMA) on ice for 60 min. Cells were washed twice and resuspended in 1% paraformaldehyde in PBS. Flow cytometric analyses were performed using a Becton Dickinson FACScan flow cytometer and FlowJo software.

2.7 Indirect Immunofluorescence

Cells were plated onto gelatin-coated coverslips or 8-well slides and fixed with ice-cold methanol for 20 min, then rinsed three times with PBS and incubated with respective primary Abs (mouse IgG, CD31, von Willebrand factor, VE-cadherin, vimentin, α-SMA) followed by species-specific FITC- or Texas Red-conjugated secondary Abs and DAPI to label nuclei. Images were taken using a 20× objective with an Axiophot II microscope (Zeiss, Oberkochen, Germany) equipped with AxioCam MRc5 (Zeiss).

2.8 Quantitative Reverse Transcriptase PCR (qPCR)

RNA was extracted and cDNA prepared as described [42]. Primers used are listed in Supplemental Table 1. All reactions were performed using Fast start SYBR Green PCR Master Mix, at the default setting on an ABI Biosystems StepOnePlus Real Time PCR Machine with the following temperature profiles: denature at 95°C for 10 minutes, and 3 cycles of 95°C for 15 sec, and 60°C for 1 min. All PCR products were sequenced using ABI DNA sequencer (Dana Farber/Harvard Cancer Center DNA Resource core) to verify the sequence corresponded to the gene of interest. Amplification efficiencies for all genes were

between 90–110%. Standard curves were generated, for relative quantification, and results were normalized to either to β–actin or ribosomal protein S9 levels.

2.9 Western Blots

Cells were lysed and analyzed by western blot as described [9, 42]. Membranes were incubated with respective primary Abs (goat anti-human CD31, goat antihuman VE-cadherin, mouse anti-bovine eNOS, mouse anti-human α-SMA, and mouse antihuman β-actin) and with secondary Ab (peroxidase-conjugated anti-mouse or anti-goat). Expression was quantified via densitometric analysis. In brief, pixel intensity of each lane was quantified in ImageJ, with background intensity subtracted from each lane. Pixel intensity for each lane was then normalized to intensity of the loading control, β-actin.

2.10 Functional Assays

Leukocyte Adhesion—Leukocyte adhesion after exposure to inflammatory cytokines was used as an indicator of endothelial function. VEC monolayers were treated ±TGFβ1 and ± CM as indicated in 35 mm culture plates. Following treatment, cells were challenged ± 10 ng/ml of TNF-α for 5 hours to induce expression of leukocyte adhesion molecules. The human myeloid cell line HL-60 (2×10^6 cells) was added and incubated at 4°C in HL-60 media (RPMI1640 media with 20% FBS and 1% GPS) on a rocking platform for 45 min. Monolayers were washed five times with cold RPMI1640 media and fixed with 4% paraformaldehyde for 30 minutes. Adherent leukocytes were visualized and quantified using a phase-contrast microscope and ImageJ analysis software.

Collagen Gel Contraction Assay—Contractile activity was measured to assess the myofibroblastic or activated phenotype of VIC. Cells were plated in 6-well plates and/or in Transwells and cultured for 5 days with specified treatment. After 5 days, cells were trypsinized and seeded into collagen gels (3 mg/ml type I collagen, DMEM, 25mM HEPES, titrated to pH 7.3 with 1M NaOH). Gels were prepared at a volume of 0.5ml gel/well and allowed to polymerize for one hour at 37°C. Following one hour, 1ml of EBM-B was added to each well, and gels were released from the sides of the plate with a 27-gauge needle. At time points indicated, the free floating gels were imaged using a camera and surface areas were calculated using ImageJ. The surface areas of free-floating gels without cells were used as control.

2.11 ^{3}H Proline Incorporation as a Measure of Collagen Biosynthesis

Cells were plated in 96 well plates at a density of 10,000 cells/well in EBM-B. After 24 h, cells were treated with proline free media (DMEM, 1% GPS) for 30 min, and washed 3×5 min with PBS. 1uCi of ^{3}H proline was added per well, in proline-free DMEM, 1% GPS, 50ug/ml L-ascorbic acid. Cell supernatants were collected and protein was precipitated with 10% trichloroacetic acid and pelleted by centrifugation at 14,000 rpm for 30 min. The pellet was suspended in 0.3 ml of 0.3 M NaOH/0.3% SDS and incubated at 37 °C for one hour until solubilized, and added to 4 ml of liquid scintillation fluid. Cell associated collagen was quantified by washing the cell monolayers with PBS, removing cells from the plate with trypsin and precipitating with 1 ml of ice-cold 10% trichloroacetic acid. The precipitate was solubilized at 37 °C for 1h in 0.3 ml of 0.3M NaOH/0.3% SDS and added to 4 ml of liquid

scintillation fluid. The acid precipitated (protein incorporated) ^{3}H counts were detected using a Perkin Elmer Tri-Carb2900TR liquid scintillation analyzer.

2.12 Cellular Proliferation Assay

Cells were plated at 10,000 cells/cm^2 in 96 well gelatin-coated plates in EBM-B, in triplicate. The next day the media was changed to EGM-2, 1% FBS, 1% GPS to serum-starve overnight. The following day, EBM-2 media was added back +/− 10ng/ml VEGF-A. Seventy-two hours later the Cell Titer96 Aqueous One Cell Proliferation Assay (MTS) reagent was added and absorbance at 490 nm was measured.

2.13 Statistical Analyses

qPCR data were analyzed as means ± standard deviation; values were normalized to the control, which was set = 1.0, so that results from three separate experiments could be compiled. Data were analyzed by two-tailed t-tests assuming unequal variance, with p value <0.05 considered significant.

HL-60 cell adhesion was analyzed as the average number of leukocytes adhered per cell, averaged over ten randomly selected visual fields of (100um × 100um). Data is expressed as mean +/− standard deviation. Statistical significance was determined using the one tailed Student's t-test, assuming unequal variance, with p value <0.05 considered significant.

Gel contraction data was compiled as the average of three gels per experiment. Data were analyzed using the two-tailed Student's t-test, assuming unequal variance, with p value <0.05 considered significant.

3. Results

3.1 Mitral VEC and VIC

The mitral VEC clones used in this study, C4, C5 and E10, were previously characterized and shown to undergo TGFβ-mediated EndMT [9]. Ovine mitral VIC are characterized in Figure 1. We analyzed ovine mitral VIC from the primary culture (primary) and five mitral VIC clones for expression of the endothelial marker VE-cadherin and the activated VIC marker α-SMA (Figure 1A). Mitral VEC clone E10 was analyzed in parallel as a positive and negative control, respectively, for VE-cadherin and α-SMA. Mitral VIC clones VIC-7, VIC-K5, and VIC-K19 did not express VE-cadherin whereas the primary VIC and clones VIC-B12 and -G8 showed low expression, perhaps indicative of the endothelial origin of VIC [12]. The VIC primary culture and the five VIC clones were positive for α-SMA, indicating an activated phenotype, as expected. VE-cadherin was not detected in the mitral VIC primary culture or in clone VIC-B12 by immunofluorescence (Figure 1B; BM-MSC served as a negative control while mitral VEC-C5 served as a positive control (Figure 1C). α-SMA and vimentin were detected in mitral VIC primary cells and clone VIC-B12 by immunofluorescence, further confirming the VIC phenotype. Mitral VEC C5 stained positive for endothelial markers CD31 and VE-Cadherin, but not for α-SMA (Figure 1C), as expected. The mitral VIC expressed VEGF-A, basic fibroblast growth factor and produced collagen, as measured by ^{3}H-proline incorporation (Supplemental Figure 1A).

3.2 Mitral VIC inhibit TGFβ1-induced EndMT in VEC

We used indirect co-culture to determine if mitral VIC produce factors that can diffuse across the 0.4 μm filter of the Transwell™ and block EndMT. Mitral VEC, clone C5 or E10, were plated in bottom chambers and mitral VIC-7 were plated in upper chambers on Day 0 and cultured for 24 hours, separately, to allow cell attachment to occur without influence from the other cell type. After 24 hours, the upper chambers were moved onto the bottom chambers containing VEC (Figure 2A). Cultures were treated without or with $TGF\beta_1$ for 4 days, at which time the EndMT markers Slug, Snai1 and matrix metalloproteinase (MMP)-2 were analyzed by qPCR. In addition, NFATc1, a transcription factor expressed in endocardial cushion cells that has been shown to mark cells that do not undergo EndMT [43, 44], was also measured (Figure 2B). $TGF\beta_1$ caused a marked induction of Slug, Snai1 and MMP-2 and a reduction in NFATc1, as previously reported [45]. Co-culture with VIC resulted in a statistically significant reduction in TGFβ1-induced Slug, Snai1 and MMP-2 and a statistically significant increase in NFATc1. Co-culture with VIC in the absence of TGFβ had no effect on the expression of these markers.

We also analyzed the EndMT marker α-SMA and the endothelial marker VE-cadherin by Western blot in VEC clone C5: co-culture with primary mitral VIC inhibited the $TGF\beta_1$ induced expression of α-SMA (Figure 1C). The same experiment was performed except that conditioned media (CM) from the primary culture of mitral VIC was placed in the upper chamber instead of VIC (Figure 2D). VEC were analyzed after 5 days and 8 days. CM added from Day 5–8 only was sufficient to reduce α-SMA in cells treated from Day 1–8 with $TGF\beta_1$, indicating that the CM was effective even when added 5 days after $TGF\beta_1$ had been added. eNOS levels were maintained, indicating a healthy endothelial phenotype. The reduction in α-SMA in VEC treated with $TGF\beta_1$ was confirmed with three different mitral VEC clones and with three different VIC, as well as CM from three different VIC (Supplemental Figure 2A). In Figure 2E, quantification of α-SMA levels in TGFβ-treated VEC are shown for three sets of co-culture experiments: VEC co-cultured with VIC primary cells (black bars), VEC co-cultured with VIC clone B12 (gray bars) and VEC co-cultured with VIC B12 CM (white bars). A statistically significant decrease in α-SMA was observed in the VEC in each co-culture setting.

In a previous study, we showed human pulmonary VEC that underwent TGFβ-mediated EndMT lost their ability to upregulate leukocyte adhesion molecules and bind leukocytes [11], a critical endothelial function. Therefore, we tested whether VIC CM could prevent a similar loss in $TGF\beta_1$-treated mitral VEC. We treated the mitral VEC for 5 days as follows: EBM-B alone, EBM-B + CM-VIC, EBM-B + $TGF\beta_1$, EBM-B + CM-VIC + $TGF\beta_1$. All four cell cultures were stimulated with TNFα for four hours to induce expression of leukocyte adhesion molecules (VCAM-1, ICAM-1 and E-selectin). HL-60 cells were added to each treatment group for 45 minutes. $TGF\beta_1$ pre-treatment for 5 days abolished HL-60 cell adherence to the TNF-α-stimulated VEC monolayer ($p<0.05$) indicating a loss of a vital endothelial cell function due to EndMT. Concomitant treatment with CM from VIC significantly restored HL-60 cell adhesion to the VEC monolayer ($p<0.05$) (Figure 2E). Leukocyte adhesion in VEC treated with CM in the absence of $TGF\beta_1$ was not significantly

different from the control (p=0.22). In summary, the results in Figure 2 show that co-culture with VIC or CM from VIC maintains an endothelial phenotype.

3.3 Mitral VEC reverse the activated VIC phenotype

We used co-culture in Transwell™ plates again to examine the effect of mitral VEC on VIC (Figure 3A). Mitral VIC clone B12 or primary VIC exposed to VEC co-culture for 5 days showed a dramatic reduction in α-SMA (Figure 3B). Quantification of the α-SMA band intensities relative to β-actin in VIC exposed to CM from VEC clones C5 and C4 is shown in Figure 3C. Statistically significant decreases in α-SMA were observed in both cases (n=3 for each). Corresponding western blots are shown in Supplemental Figure 3. The ability of VEC to reduce the activated VIC phenotype was confirmed by analyzing expression of α-SMA and SM22-α, another myofibroblast marker [46], by indirect immunofluorescence (Figure 3D). The percent α-SMA positive cells was reduced from 63% to 17% in VIC co-cultured with VEC while the percent SM22-α positive cells was reduced from 100% to 32% in VIC co-cultured with VEC (Figure 3D, bar graphs).

We next analyzed expression of type I collagen and Chm1 mRNA by qPCR in VIC co-cultured with VEC or CM from VEC for 3 days, as in Fig 3A. Type I collagen is increased in activated VIC; it is not expressed by VEC [6]. Chm1 is expressed in VIC in vivo and in vitro. Loss of Chm1 in cardiac valves leads to increased angiogenesis and valve degeneration [13, 24]. Thus, we use Chm1 as an indicator of a quiescent healthy VIC phenotype. We tested the effects of two different mitral VEC clones and CM from three different mitral VEC on primary mitral VIC. The results of these experiments show that co-culture of VIC with VEC or CM from VEC significantly decreased collagen I (VIC + VEC, $p = 0.03$, VIC + CM-VEC $p = 0.02$) and significantly increased Chm1 mRNA (VIC + CM-VEC $p = 0.03$) (Figure 3E). This finding indicates that mitral VEC can promote the quiescent VIC phenotype.

In Figure 3F, we tested the reversibility of the quiescent VIC state by treating VIC with CM-VEC for three days, and then either continuing to culture the cells in CM-VEC for two additional days, or removing the CM and replacing with EBM-B for 2 days. Lanes 1 and 3 show high levels of α-SMA in VIC cultured without CM at day 3 and 5. Lanes 2 and 4 show the suppression of α-SMA in VIC exposed to CM-VEC. In contrast, VIC treated for 3 days with CM-VEC followed by 2 days in EBM-B showed a restored level of α-SMA (lane 5 and bar graph). This indicates that the quiescent VIC phenotype requires continuous signal from the VEC when the VIC are grown on tissue culture dishes in EBM-B. As a control, we analyzed CM from VEC and VIC for effects on basal and VEGF-induced proliferation of VEC and VIC (Supplemental Figure 4A, B); no significant effects were observed.

3.4 Contractile activity of mitral VIC is reduced by co-culture with VEC

We measured contractility of VIC to assess cellular function in response to VEC. The free-floating collagen gel assay in which VIC were seeded on a collagen gels and allowed to contract the gels, is described in materials and methods. The gel surface area was measured over time, and plotted as percent reduction in gel area as an indication of contractile activity (Figure 4A–B). We optimized the assay (Supplemental Figure 4A) and tested a panel of

cells including mitral VIC, VEC, and endothelial colony forming cells (ECFC) (Figure 4B). The endothelial cells (mitral VEC-E10 and ECFC) exhibited little to no contractile behavior while three mitral VIC contracted the free floating collagen gels, consistent with myofibroblast-like function. All three of the mitral VIC clones in Figure 4B tested positive for α-SMA expression, which confirmed their activated VIC phenotype. TGFβ treatment to further increase VIC activation resulted in increased contraction (Supplemental Figure 4B), providing validation of the gel contraction assay [22].

We hypothesized that the reduction in VIC α-SMA and SM22α observed when VIC were co-cultured with VEC would correlate with a reduction in contractile activity of the mitral VICs, as there is evidence in the literature that α-SMA and SM22α play a role in cell contractility in smooth muscle cells [47]. To test this, VIC were treated with CM-VEC for 5 days (n=3) and then seeded in the collagen gel contraction assay. Gel contraction was measured at one hour (Figure 4C). CM from three different mitral VEC clones (C4, C5 and E10) significantly reduced the contractile activity of the primary VIC ($p=0.02$, $p=0.001$, $p=0.006$ for treatment with CM VEC-C4, VEC-C5, and VEC-E10, respectively).

3.5 Non-valvular Endothelial and Mesenchymal Cells

We used ovine BM-MSC to determine if a non-valvular mesenchymal cell could inhibit $TGF\beta_1$ induced EndMT in the mitral VEC. CM from BM-MSC inhibited TGFβ-induced EndMT in the mitral VEC C5 (Figure 5A). As a control, we tested whether CM from endothelial cells would inhibit TGFβ-induced EndMT. Endothelial CM from ECFC did not inhibit TGFβ-induced EndMT in mitral VEC (Figure 5B).

We also tested the ability of non-valvular endothelial cells, ECFC and carotid artery endothelial cells (CAEC), to suppress the activated VIC phenotype in the Transwell assay, as described in Figure 3A. ECFC and CAEC were similar in ability to induce a quiescent, α-SMA-low VIC phenotype (Figure 5C, gray bars). In a second arm of the experiment, VIC were treated with $TGF\beta_1$ to enhance the activated state of the VIC [23]. $TGF\beta_1$-treated VIC did not respond to co-culture with ECFC, mitral VEC clone D6 or CAEC in that α-SMA protein expression was not reduced (Figure 5C, black bars). This indicates that $TGF\beta_1$ renders the VIC not only activated but resistant to soluble factors produced by endothelial cells. In Figure 5D, we showed that CM from mitral VEC or from CAEC was sufficient to suppress α-SMA in primary VIC. We tested the ability of the non-valvular endothelial cells to inhibit VIC function in the collagen gel contraction assay. CM from ECFCs showed a similar ability to reduce VIC contraction as CM from mitral VEC (Supplemental Figure 4C). This set of experiments indicates 1) that TGFβ-mediated EndMT in mitral VEC can be prevented by CM from mesenchymal stem cells but not from endothelial cells and 2) the activated VIC phenotype can be suppressed by co-culture with non-valvular endothelial cells or with CM from non-valvular endothelial cells. This apparent lack of restriction to valve-derived cells suggests that it may be possible to use non-valvular cell sources to modulate these cellular events in valve diseases.

4. Discussion

Our study shows that mitral VIC produce soluble factor(s) that diminish TGFβ-mediated EndMT in mitral VEC. The reduced EndMT was shown by decreased expression of EndMT markers and retention of a critical endothelial function - leukocyte adhesion. In turn, mitral VEC produce soluble factor(s) that dampen the myofibroblastic, activated properties of mitral VIC in culture. Mitral VIC co-cultured with VEC or conditioned media from VEC showed decreases in three hallmarks of myofibroblast-like, activated VIC –α-SMA, collagen I, and ability to contract collagen gels, and further, showed an increase in chondromodulin-1 (Chm1), a marker of healthy VIC. Bone marrow-derived mesenchymal stem cells, cells that share some differentiative and phenotypic properties with VIC [48], were also able to mitigate TGFβ-driven EndMT in VEC. Furthermore, we found that two types of non-valvular endothelial cells – ECFC and CAEC – were able to reduce the myofibroblastic phenotype of mitral VICs. These findings indicate that the ability to modulate these cellular activities is not restricted to valve-derived endothelial and interstitial cells.

Our results show that cellular phenotypes found in healthy valves can be reconstituted, or at least approximated, when VEC and VIC are co-cultured without direct cell-cell contact using Transwell™ inserts. The α-SMA-positive phenotype observed in VIC grown on tissue culture plastic dishes has been attributed to the artificial nature of the in vitro setting. Our data indicate that a critical aspect of this artificial setting is the *absence* of endothelial cells. This in vitro finding fits well with the concept that the onset of activated VIC in vivo could arise from a disrupted or dysfunctional endothelium.

There are several limitations to our study. The first is that other factors besides TGFβ, such as low steady sheer stress and oscillatory shear stress [49], pathological cyclic strain [18], TNFα and IL-6 [19] can induce EndMT. Whether or not VIC or conditioned media from VIC would be able to prevent EndMT caused by these stimuli was not tested. A second limitation is that although we attempted to identify factors produced by the VICs that are responsible for blocking the TGFβ-mediated EndMT, negative results were obtained. We investigated VEGF-A as a potential mediator because it is known to inhibit VEC EndMT, and is produced by the VIC (Supplemental Figure 1). Avastin, an anti-human VEGF-A antibody, failed to reverse the VIC mediated inhibition of EndMT, however additional experiments are needed to determine if ovine VEGF-A is recognized by Avastin. We also tested the possibility that heparin-binding (HB)-EGF produced by VIC might inhibit EndMT by adding CRM197, a recombinant protein that binds to HB-EGF and blocks its function [50, 51]. Again negative results were obtained but binding of CRM197 to ovine HB-EGF could not be ascertained. A third possibility that was not tested was whether VIC secrete a factor that increases fibroblast growth factor signaling in the VEC as this could render the cells EndMT resistant [52]. Basic fibroblast growth factor is both present in the EBM-B media used to culture VEC, and is expressed by VIC (Supplemental Figure 1) but one might speculate that a factor produced by VIC could act downstream of the growth factor to stimulate FGF-receptors or downstream signaling molecules that could, in turn, reduce the ability of the EC to respond to TGFβ [52]. It will be important to determine the nature and

identify of the secreted factors and the mechanisms by which they prevent EndMT in future studies.

Based on previous studies on aortic valves, a likely mediator released by the VECs to dampen the VIC activated phenotype is nitric oxide. Using a similar Transwell co-culture system, Bosse and colleagues showed that murine EC from endothelial nitric oxide synthase-knockout mice (NOS3−/−) were unable to block calcification in aortic VEC, but over expression of NOS3 in EC restored the activity [36]. Two groups showed a reduction in α-SMA, when porcine aortic VEC were directly co-cultured with porcine VIC [53, 54], which was then blocked by the eNOS inhibitor L-NG-Nitroarginine Methyl Ester (L-NAME) [53]). NO released from VECs has been shown to decrease the myofibroblast-like and calcific phenotype in VICs [55]. One study reported only a small decrease in α-SMA in VICs when cells were in direct contact on tissue culture plastic, but observed a more significant decrease when cells were plated on a softer hydrogel substratum [54]. These differences in VIC responses could be due the variation in substrate stiffness, as indicated in previous studies [20, 21, 56]. It may be that VICs, in a more biocompatible setting, are more responsive to VEC influence. In summary, NO as a mediator of VIC phenotype has been increasingly reported in the literature. Another potential regulatory factor within VEC is endogenous TGFβ1, which has been shown to be expressed in murine and human valvular endothelium [57–59]. When and if endogenous VEC TGFβ plays a role in the reciprocal interactions between VEC and VIC would be an important topic to explore in the future.

In summary, our study demonstrates reciprocal interactions between mitral VEC and VIC that sustain endothelial phenotype and function in TGFβ-exposed VEC and promote a quiescent, non-contractile phenotype in VIC. The precise nature of the reciprocal interactions must be determined but our data indicate that direct cell-cell contact between VEC and VIC is not required but instead soluble factors produced by each cell type act in a paracrine manner. We speculate that disruption of these interactions may underlie the EndMT and activated VIC that appear in many types of valve disease. We further speculate that the disruptions may be caused by any number of disturbances to normal hemostasis such that the production of one or more of the putative paracrine factors is halted or altered. Further, restoration of VEC-VIC interaction in diseased valves may be achieved by supplementation or delivery of non-valvular EC and non-valvular mesenchymal cells to the damaged leaflets or cusps. Additional studies will be needed to test these concepts.

Supplementary Material

Refer to Web version on PubMed Central for supplementary material.

Acknowledgements

The authors thank Ms. Kristin Johnson for preparation of the figures.

Sources of Funding

Research reported in this manuscript was supported by the NHLBI of the National Institutes of Health under award number R01HL109506-01A1, to R.A.L. and J.B. The content is solely the responsibility of the authors and does not necessarily represent the official views of the National Institutes of Health. The study was also supported Fondation Leducq Transatlantic Network (R.A.L and J.B) and the Tommy Kaplan Discretionary Fund (J.E.M.)

Abbreviations used are

EndMT	endothelial to mesenchymal transition
VEC	valve endothelial cells
VIC	valve interstitial cells
qPCR	quantitative reverse transcriptase polymerase chain reaction
TGFβ	transforming growth factor β
α-SMA	α-smooth muscle actin
Chm1	chondromodulin-1
EBM	endothelial basal media
eNOS	endothelial nitric oxide synthase
BM-MSCs	bone marrow-derived mesenchymal stem cells
BSA	bovine serum albumin
CAECs	carotid artery endothelial cells
CM	conditioned media
ECFC	endothelial colony forming cells
ECM	extracellular matrix
FBS	fetal bovine serum
FITC	fluorescein isothiocyanate
MMP	matrix metalloproteinase
VE-Cadherin	vascular endothelial cadherin

Glossary

Endothelial to mesenchymal transition (EndMT)	the process by which endothelial cells lose their polarity and cell-cell contacts, gain migratory properties, and differentiate into mesenchymal cells. This process is essential for heart valve development.

References

1. Grande-Allen KJ, et al. Mitral valve stiffening in end-stage heart failure: evidence of an organic contribution to functional mitral regurgitation. The Journal of thoracic and cardiovascular surgery. 2005; 130(3):783–790. [PubMed: 16153929]
2. Grande-Allen KJ, et al. Apparently normal mitral valves in patients with heart failure demonstrate biochemical and structural derangements: an extracellular matrix and echocardiographic study. Journal of the American College of Cardiology. 2005; 45(1):54–61. [PubMed: 15629373]
3. Dal-Bianco JP, et al. Active adaptation of the tethered mitral valve: insights into a compensatory mechanism for functional mitral regurgitation. Circulation. 2009; 120(4):334–342. [PubMed: 19597052]

4. Aikawa E, et al. Human semilunar cardiac valve remodeling by activated cells from fetus to adult: implications for postnatal adaptation, pathology, and tissue engineering. Circulation. 2006; 113(10): 1344–1352. [PubMed: 16534030]
5. Liu AC, Joag VR, Gotlieb AI. The emerging role of valve interstitial cell phenotypes in regulating heart valve pathobiology. Am J Pathol. 2007; 171(5):1407–1418. [PubMed: 17823281]
6. Flanagan TC, et al. Reference models for mitral valve tissue engineering based on valve cell phenotype and extracellular matrix analysis. Cells Tissues Organs. 2006; 183(1):12–23. [PubMed: 16974091]
7. Hinton RB, Yutzey KE. Heart valve structure and function in development and disease. Annu Rev Physiol. 2011; 73:29–46. [PubMed: 20809794]
8. Bischoff J, Aikawa E. Progenitor cells confer plasticity to cardiac valve endothelium. J Cardiovasc Transl Res. 2011; 4(6):710–719. [PubMed: 21789724]
9. Wylie-Sears J, et al. Mitral valve endothelial cells with osteogenic differentiation potential. Arterioscler Thromb Vasc Biol. 2011; 31(3):598–607. [PubMed: 21164078]
10. Paranya G, et al. Aortic valve endothelial cells undergo transforming growth factor-beta-mediated and non-transforming growth factor-beta-mediated transdifferentiation in vitro. Am J Pathol. 2001; 159(4):1335–1343. [PubMed: 11583961]
11. Paruchuri S, et al. Human pulmonary valve progenitor cells exhibit endothelial/mesenchymal plasticity in response to vascular endothelial growth factor-A and transforming growth factor-beta2. Circ Res. 2006; 99(8):861–869. [PubMed: 16973908]
12. Lincoln J, Yutzey KE. Molecular and developmental mechanisms of congenital heart valve disease. Birth Defects Res A Clin Mol Teratol. 2011; 91(6):526–534. [PubMed: 21538813]
13. Yoshioka M, et al. Chondromodulin-I maintains cardiac valvular function by preventing angiogenesis. Nat Med. 2006; 12(10):1151–1159. [PubMed: 16980969]
14. Rabkin-Aikawa E, et al. Dynamic and reversible changes of interstitial cell phenotype during remodeling of cardiac valves. J Heart Valve Dis. 2004; 13(5):841–847. [PubMed: 15473488]
15. Stephens EH, et al. Significant changes in mitral valve leaflet matrix composition and turnover with tachycardia-induced cardiomyopathy. Circulation. 2009; 120(11 Suppl):S112–S119. [PubMed: 19752355]
16. Dvorin EL, et al. Human pulmonary valve endothelial cells express functional adhesion molecules for leukocytes. J Heart Valve Dis. 2003; 12(5):617–624. [PubMed: 14565715]
17. Jang GH, et al. Differential functions of genes regulated by VEGF-NFATc1 signaling pathway in the migration of pulmonary valve endothelial cells. FEBS Lett. 2010; 584(1):141–146. [PubMed: 19914243]
18. Balachandran K, Sucosky P, Yoganathan AP. Hemodynamics and mechanobiology of aortic valve inflammation and calcification. Int J Inflam. 2011; 2011:263870. [PubMed: 21760982]
19. Mahler GJ, Farrar EJ, Butcher JT. Inflammatory cytokines promote mesenchymal transformation in embryonic and adult valve endothelial cells. Arterioscler Thromb Vasc Biol. 2013; 33(1):121–130. [PubMed: 23104848]
20. Quinlan AM, Billiar KL. Investigating the role of substrate stiffness in the persistence of valvular interstitial cell activation. J Biomed Mater Res A. 2012; 100(9):2474–2482. [PubMed: 22581728]
21. Duan B, et al. Stiffness and Adhesivity Control Aortic Valve Interstitial Cell Behavior within Hyaluronic Acid Based Hydrogels. Acta Biomater. 2013
22. Walker GA, et al. Valvular myofibroblast activation by transforming growth factor-beta: implications for pathological extracellular matrix remodeling in heart valve disease. Circ Res. 2004; 95(3):253–260. [PubMed: 15217906]
23. Geirsson A, et al. Modulation of transforming growth factor-beta signaling and extracellular matrix production in myxomatous mitral valves by angiotensin II receptor blockers. Circulation. 2012; 126 Suppl 1(11):S189–S197. [PubMed: 22965982]
24. Hakuno D, et al. Periostin advances atherosclerotic and rheumatic cardiac valve degeneration by inducing angiogenesis and MMP production in humans and rodents. J Clin Invest. 2010; 120(7): 2292–2306. [PubMed: 20551517]
25. Chester AH. Endothelin-1 and the aortic valve. Curr Vasc Pharmacol. 2005; 3(4):353–357. [PubMed: 16248778]

26. Chester AH, Misfeld M, Yacoub MH. Receptor-mediated contraction of aortic valve leaflets. J Heart Valve Dis. 2000; 9(2):250–254. discussion 254-5. [PubMed: 10772043]
27. Cushing MC, et al. Fibroblast growth factor represses Smad-mediated myofibroblast activation in aortic valvular interstitial cells. FASEB J. 2008; 22(6):1769–1777. [PubMed: 18218921]
28. Miyamoto S, et al. A novel anti-human HB-EGF monoclonal antibody with multiple antitumor mechanisms against ovarian cancer cells. Clin Cancer Res. 2011; 17(21):6733–6741. [PubMed: 21918176]
29. Moustakas A, et al. Mechanisms of TGF-beta signaling in regulation of cell growth and differentiation. Immunol Lett. 2002; 82(1–2):85–91. [PubMed: 12008039]
30. Bajaj P, et al. Stiffness of the substrate influences the phenotype of embryonic chicken cardiac myocytes. J Biomed Mater Res A. 2010; 95(4):1261–1269. [PubMed: 20939058]
31. Butcher JT, Nerem RM. Valvular endothelial cells regulate the phenotype of interstitial cells in co-culture: effects of steady shear stress. Tissue Eng. 2006; 12(4):905–915. [PubMed: 16674302]
32. Ku CH, et al. Collagen synthesis by mesenchymal stem cells and aortic valve interstitial cells in response to mechanical stretch. Cardiovasc Res. 2006; 71(3):548–556. [PubMed: 16740254]
33. Waxman AS, et al. Interactions between TGFbeta1 and cyclic strain in modulation of myofibroblastic differentiation of canine mitral valve interstitial cells in 3D culture. J Vet Cardiol. 2012; 14(1):211–221. [PubMed: 22386586]
34. El-Hamamsy I, et al. Endothelium-dependent regulation of the mechanical properties of aortic valve cusps. J Am Coll Cardiol. 2009; 53(16):1448–1455. [PubMed: 19371829]
35. Lupu F, Simionescu M. Organization of the intercellular junctions in the endothelium of cardiac valves. J Submicrosc Cytol. 1985; 17(2):119–132. [PubMed: 3999177]
36. Bosse K, et al. Endothelial nitric oxide signaling regulates Notch1 in aortic valve disease. Journal of molecular and cellular cardiology. 2013; 60:27–35. [PubMed: 23583836]
37. Richards J, et al. Side-specific endothelial-dependent regulation of aortic valve calcification: interplay of hemodynamics and nitric oxide signaling. The American journal of pathology. 2013; 182(5):1922–1931. [PubMed: 23499458]
38. El Accaoui RN, et al. Aortic Valve Sclerosis in Mice Deficient in Endothelial Nitric Oxide Synthase. American journal of physiology. Heart and circulatory physiology. 2014
39. Kaushal S, et al. Functional small-diameter neovessels created using endothelial progenitor cells expanded ex vivo. Nat Med. 2001; 7(9):1035–1040. [PubMed: 11533707]
40. Melero-Martin JM, et al. Engineering robust and functional vascular networks in vivo with human adult and cord blood-derived progenitor cells. Circ Res. 2008; 103(2):194–202. [PubMed: 18556575]
41. Bucala R, et al. Circulating fibrocytes define a new leukocyte subpopulation that mediates tissue repair. Mol Med. 1994; 1(1):71–81. [PubMed: 8790603]
42. Wylie-Sears J, Levine R, Bischoff J. Losartan Inhibits Endothelial-to-Mesenchymal Transformation in Mitral Valve Endothelial Cells by Blocking Transforming Growth Factor-beta-induced Phosphorylation of ERK. Biochemical and biophysical research communications. 2014
43. Wu B, et al. Nfatc1 coordinates valve endocardial cell lineage development required for heart valve formation. Circulation Research. 2011; 109(2):183–192. [PubMed: 21597012]
44. Wu B, Baldwin HS, Zhou B. Nfatc1 directs the endocardial progenitor cells to make heart valve primordium. Trends in Cardiovascular Medicine. 2013; 23(8):294–300. [PubMed: 23669445]
45. Wylie-Sears J, Levine RA, Bischoff J. Losartan inhibits endothelial-tomesenchymal transformation in mitral valve endothelial cells by blocking transforming growth factor-beta-induced phosphorylation of ERK. Biochemical and biophysical research communications. 2014
46. Cheng SL, et al. Dkk1 and MSX2-Wnt7b signaling reciprocally regulate the endothelial-mesenchymal transition in aortic endothelial cells. Arterioscler Thromb Vasc Biol. 2013; 33(7): 1679–1689. [PubMed: 23685555]
47. Zeidan A, et al. Ablation of SM22alpha decreases contractility and actin contents of mouse vascular smooth muscle. FEBS Lett. 2004; 562(1–3):141–146. [PubMed: 15044015]

48. Chen JH, et al. Identification and characterization of aortic valve mesenchymal progenitor cells with robust osteogenic calcification potential. The American journal of pathology. 2009; 174(3): 1109–1119. [PubMed: 19218344]

49. Mahler GJ, et al. Effects of shear stress pattern and magnitude on mesenchymal transformation and invasion of aortic valve endothelial cells. Biotechnol Bioeng. 2014

50. Mitamura T, et al. Diphtheria toxin binds to the epidermal growth factor (EGF)-like domain of human heparin-binding EGF-like growth factor/diphtheria toxin receptor and inhibits specifically its mitogenic activity. J Biol Chem. 1995; 270(3):1015–1019. [PubMed: 7836353]

51. Yamazaki S, et al. Mice with defects in HB-EGF ectodomain shedding show severe developmental abnormalities. J Cell Biol. 2003; 163(3):469–475. [PubMed: 14597776]

52. Chen PY, et al. FGF regulates TGF-beta signaling and endothelial-to-mesenchymal transition via control of let-7 miRNA expression. Cell reports. 2012; 2(6):1684–1696. [PubMed: 23200853]

53. El Accaoui RN, et al. Aortic valve sclerosis in mice deficient in endothelial nitric oxide synthase. Am J Physiol Heart Circ Physiol. 2014; 306(9):H1302–H1313. [PubMed: 24610917]

54. Gould ST, et al. The role of valvular endothelial cell paracrine signaling and matrix elasticity on valvular interstitial cell activation. Biomaterials. 2014; 35(11):3596–3606. [PubMed: 24462357]

55. Richards J, et al. Side-specific endothelial-dependent regulation of aortic valve calcification: interplay of hemodynamics and nitric oxide signaling. Am J Pathol. 2013; 182(5):1922–1931. [PubMed: 23499458]

56. Stephens EH, et al. Mitral valvular interstitial cell responses to substrate stiffness depend on age and anatomic region. Acta Biomater. 2011; 7(1):75–82. [PubMed: 20624493]

57. Akhurst RJ, et al. TGF beta in murine morphogenetic processes: the early embryo and cardiogenesis. Development. 1990; 108(4):645–656. [PubMed: 1696875]

58. Gatherer D, et al. Expression of TGF-beta isoforms during first trimester human embryogenesis. Development. 1990; 110(2):445–460. [PubMed: 2133548]

59. Molin DG, et al. Expression patterns of Tgfbeta1–3 associate with myocardialisation of the outflow tract and the development of the epicardium and the fibrous heart skeleton. Developmental dynamics : an official publication of the American Association of Anatomists. 2003; 227(3):431–444. [PubMed: 12815630]

Highlights

- Quiescent valve endothelial and interstitial cell phenotypes approximated in vitro.
- Valve interstitial cells inhibited TGFβ-induced endothelial to mesenchymal transition.
- Valve endothelial cells reversed myofibroblastic phenotype of interstitial cells.

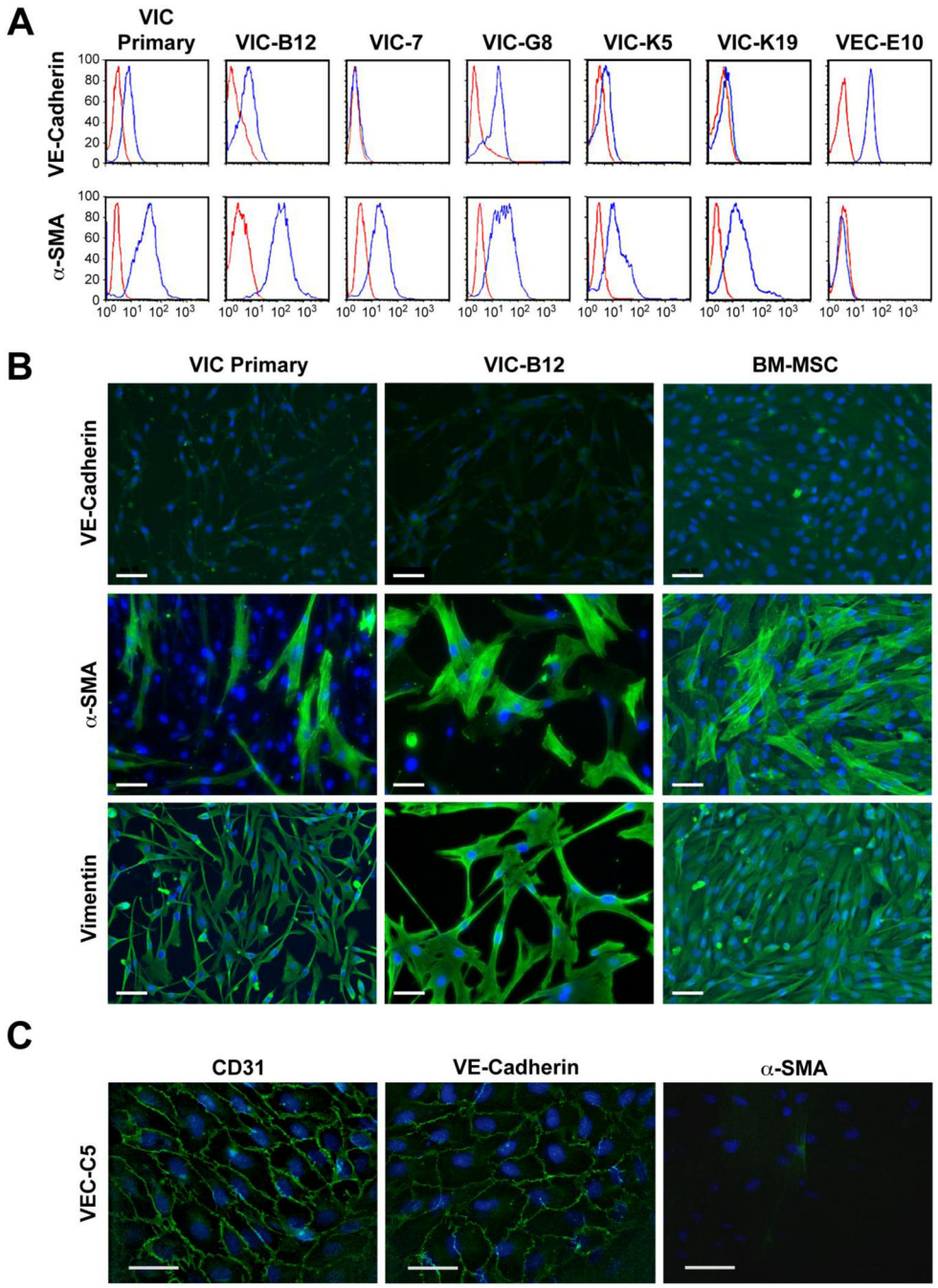

Figure 1.

Phenotype of mitral valve interstitial cells (VIC) A. Flow cytometry of VIC with anti-VE-cadherin (top row) and anti-α-SMA (bottom row) (blue lines). Red line indicates cells incubated with isotype-matched control IgG. B. Immunofluorescence staining for VE-cadherin (top row), α-SMA (middle row) and vimentin (bottom row); nuclei stained blue with DAPI. Scale bar, 50 μM. C. Mitral VEC immunostained for CD31 (left panel), VE-cadherin (middle panel) and α-SMA (right panel); nuclei stained blue with DAPI. Scale bar, 20 μM.

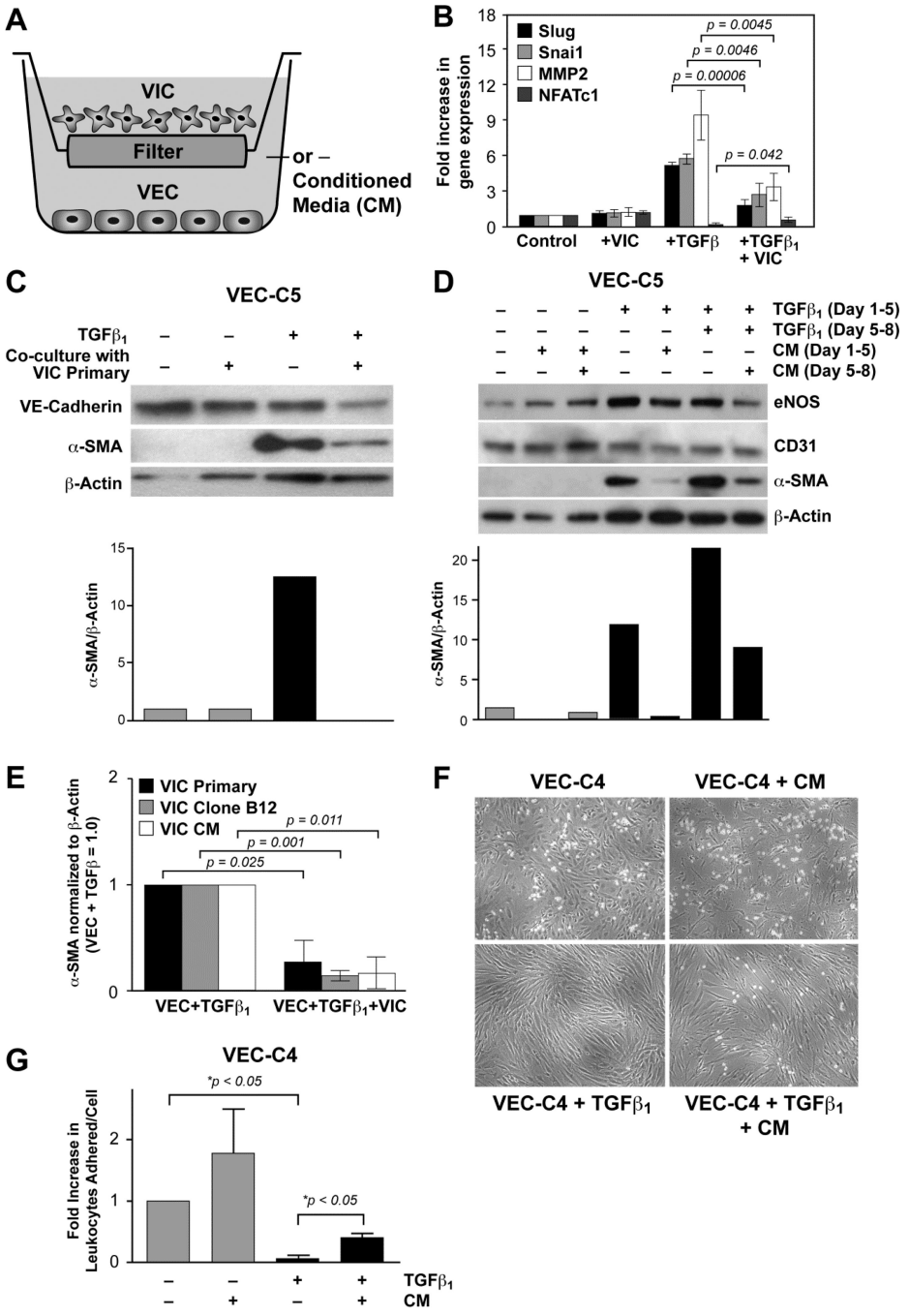

Figure 2.

VIC inhibit TGFβ1-induced EndMT in VEC A. Schematic of mitral VIC-VEC co-culture. B. qPCR of EndMT markers Slug, Snai1, MMP1 and NFATc1 in untreated mitral VEC (control), mitral VEC co-cultured with VIC (+VIC), mitral VEC treated with $TGF\beta_1$ for 4 days ($+TGF\beta_1$) and mitral VEC treated with $TGF\beta_1$ and co-cultured with VIC ($+TGF\beta_1$ + VIC). Values were analyzed by two-tailed t-tests assuming unequal variance, with p value <0.05 considered significant. C. Western blot of VEC-C5 that had been co-cultured with VIC primary cells. Bar graph shows the levels of αSMA normalized to β-actin in each lane

determined by image analysis of the western blot. D. Western blot of VEC-C5 co-cultured without (gray bars) or with TGFβ_1 (black bars) from day 1–8 and with CM from VIC primary day 5–8. eNOS and CD31 serve as endothelial markers. Levels of αSMA normalized to β-actin in each lane were determined by image analysis. E. Levels of αSMA in VECs treated with TGFβ_1 +/− co-culture with VIC primary cells (black bars), VIC clone B12 (gray bars) or VIC clone B12 CM (white bars), n=3 for each. Values were analyzed by two tailed t-tests assuming unequal variance, with p value < 0.05 considered significant. F–G. HL-60 leukocyte adhesion assay. VEC-C4 cells were treated with VIC CM, TGFβ_1 or TGFβ_1 + CM for 5 days prior to 5 hour treatment with TNF-α to induce expression of leukocyte adhesion molecules. HL-60 cells were allowed to adhere to the VEC monolayer for 45 minutes before washing with PBS. Bound HL-60 cells were photographed and counted. Data is expressed as mean +/− standard deviation. Statistical significance was determined using the one tailed Student's t-test, assuming unequal variance, with p value <0.05 considered significant.

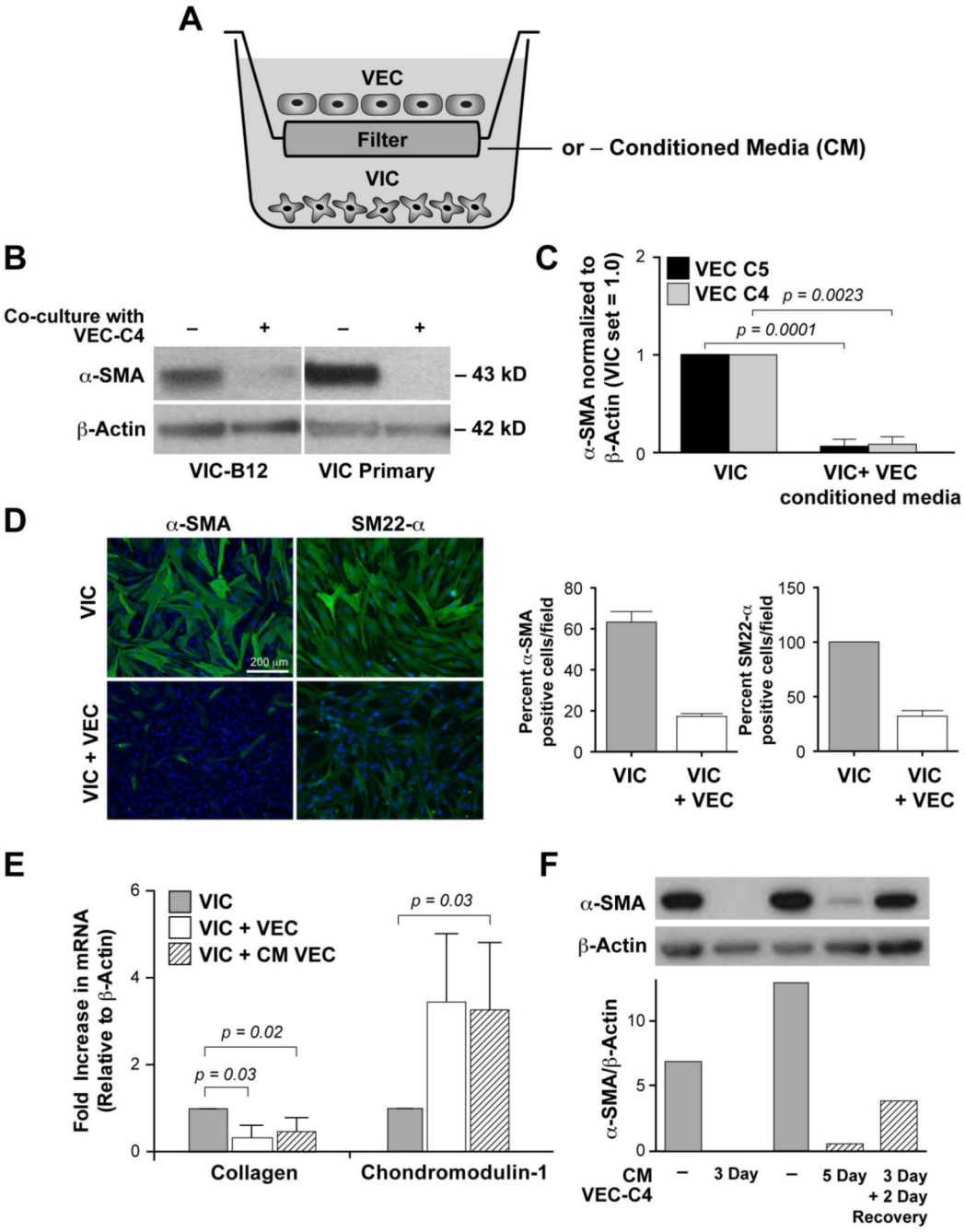

Figure 3.

VEC reduce the activated VIC phenotype. A. Schematic of VEC-VIC co-culture. B. Western blot of lysates from VIC-B12 and VIC Primary co-cultured with VEC-C4. C. Levels of αSMA in VIC were normalized to β-actin and set 1.0 and compared to levels in VIC co-cultured with CM from VEC clone C5 (black bars) or VEC clone C4 (gray bars), n=3 for each. Values were analyzed by two tailed t-tests assuming unequal variance, with p value < 0.05 considered significant. D. Immunofluorescence staining for α-SMA and SM22-α (green) in VIC and VIC co-cultured with VEC. Nuclei are stained with blue with DAPI.

Scale bar = 200 um. Bar graphs show quantification of positive cells/field. Five randomly selected fields at 20× magnification were quantified and expressed as average percent positive cells/field. E. qPCR for type I collagen and Chm1 in VIC that had been cultured alone (gray bar), indirectly with VEC (white bar) or with CM from VEC (hatched bar). Values were analyzed by one-tailed t-tests assuming unequal variance; a p value <0.05 is considered significant. F. Western blot of VIC cultured with CM from VEC-C4 as shown. Bar graph below the blots shows quantification α-SMA normalized to β-actin.

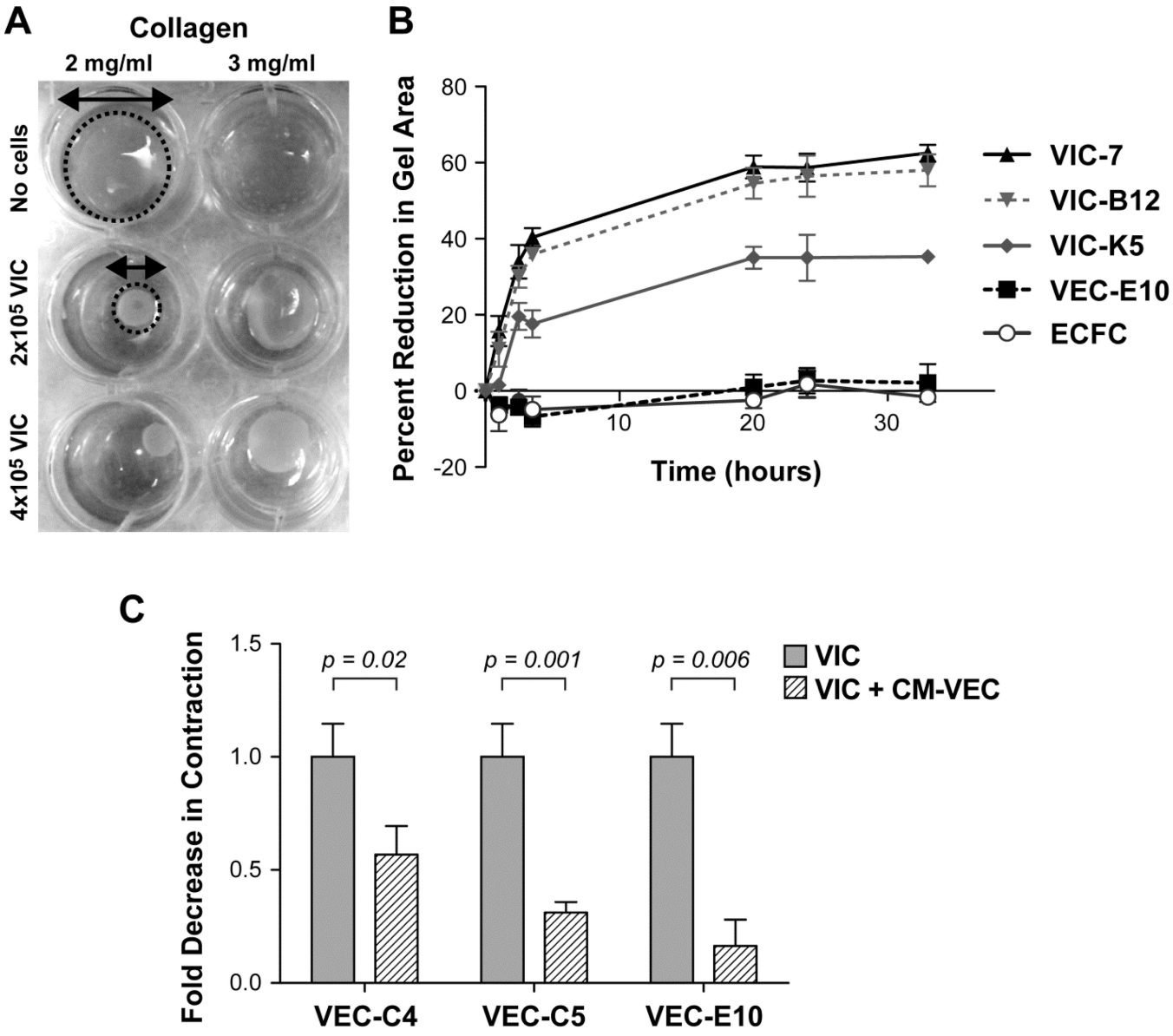

Figure 4.

VIC contractility assay A. Optimization of VIC collagen gel contraction assay. B. Three different VIC clones contracted collagen gels over time; VEC and ECFC did not. C. VIC were cultured alone (gray bar) or with CM from VEC for 5 days (hatched bar), plated on collagen gels for one hour, and percent reduction in gel area measured. Means ± standard deviation were analyzed by two-tailed t-tests assuming unequal variance; a p value <0.05 is considered significant.

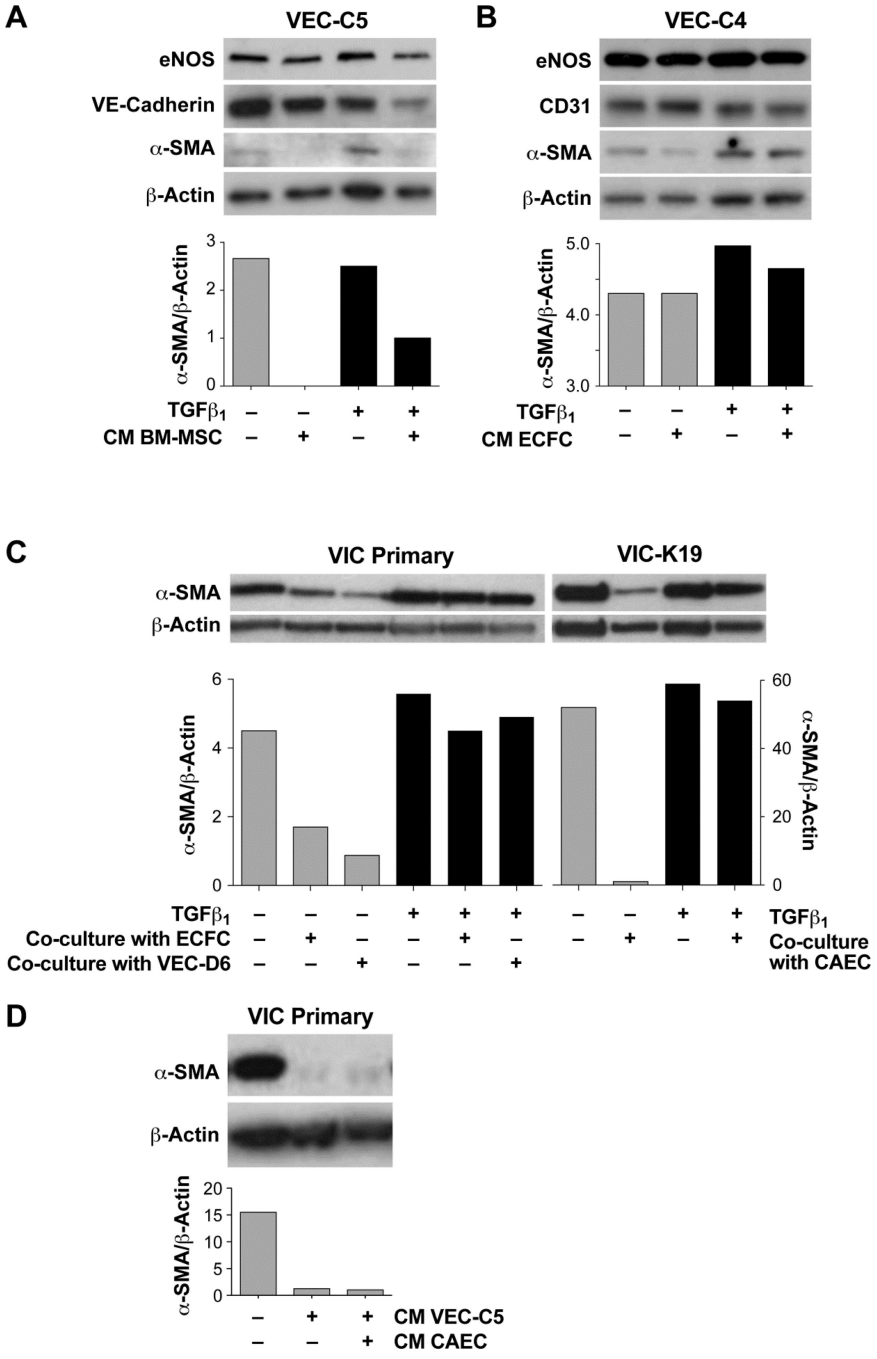

Figure 5.

A. Western blot of VEC-C5 co-cultured with CM from BM-MSC in the absence (gray bars) or presence of TGFβ_1. B. Western blot of VEC-C4 cultured with CM from ECFC in the absence (gray bars) or presence of TGFβ_1. C. Western blot of VIC Primary (left) and VIC-K19 (right) co-cultured with ECFC, VEC-D6 or with CAEC as shown. Cells were treated without (gray bars) or with TGFβ_1 for 5 days. D. Western blot of VIC primary cultured with

CM from VEC-C5 or from CAEC. Bar graph shows α-SMA band intensities normalized to β-actin.